Spectroscopic characterization of the ground and low-lying electronic states of Ga_2N via anion photoelectron spectroscopy

Sean M. Sheehan, Giovanni Meloni,[a] Bradley F. Parsons, Nadine Wehres, and Daniel M. Neumark[b]
Department of Chemistry, University of California, Berkeley, California 94720 and Chemical Sciences Division, Lawrence Berkeley National Laboratory, Berkeley, California 94720

(Received 27 October 2005; accepted 30 November 2005; published online 8 February 2006)

Anion photoelectron spectra of Ga_2N^- were measured at photodetachment wavelengths of 416 nm(2.978 eV), 355 nm(3.493 eV), and 266 nm(4.661 eV). Both field-free time-of-flight and velocity-map imaging methods were used to collect the data. The field-free time-of-flight data provided better resolution of the features, while the velocity-map-imaging data provided more accurate anisotropy parameters for the peaks. Transitions from the ground electronic state of the anion to two electronic states of the neutral were observed and analyzed with the aid of electronic structure calculations and Franck-Condon simulations. The ground-state band was assigned to a transition between linear ground states of $Ga_2N^-(X\ ^1\Sigma_g^+)$ and $Ga_2N(X\ ^2\Sigma_u^+)$, yielding the electron affinity of Ga_2N, 2.506 ± 0.008 eV. Vibrationally resolved features in the ground-state band were assigned to symmetric and antisymmetric stretch modes of Ga_2N, with the latter allowed by vibronic coupling to an excited electronic state. The energy of the observed excited neutral state agrees with that calculated for the $A\ ^2\Pi_u$ state, but the congested nature of this band in the photoelectron spectrum is more consistent with a transition to a bent neutral state. © *2006 American Institute of Physics*. [DOI: 10.1063/1.2159492]

I. INTRODUCTION

Since the development of gallium-nitride (GaN)-based blue light-emitting diodes[1,2] and laser diodes[3,4] in the 1990's, there has been increased focus in the field of optoelectronics on further developing GaN-based materials for a variety of applications, including high-density optical data storage and high-efficiency white light sources. At the same time, the emergence of nanotechnology has fueled the drive to build ever smaller electrical and optical devices based on nanostructures such as nanotubes and nanowires. Inevitably, the promise of GaN as a semiconductor, owing to its large bandgap, has led to its increased use in these novel devices. Field-effect transistors[5] as well as nanoscale lasers[6] have been fabricated based on single GaN nanowires. As devices become even smaller and confinement effects become more prominent, it is hoped that a study of the electrical properties of small clusters of GaN will lead to a better understanding of the properties of such devices.

Photoelectron (PE) spectroscopy of anions is an ideal technique to study these small clusters due to its mass selectivity and because it provides information on the structures and energetics of the neutral clusters.[7] Here we report the PE spectrum of Ga_2N^-, the first gas-phase characterization of any Ga_xN_y species. This work represents a continuation of previous work in our group on III–V semiconductor clusters.[8–11]

There have been numerous theoretical studies on small clusters of gallium nitride with particular emphasis on the stoichiometric clusters $(Ga_xN_x, x=1-6)$.[12–20] Less attention has been paid to nonstoichiometric clusters.[21–26] Costales *et al.*[23] studied the evolution of the N–N bond in metal-rich Ga_nN_2 $(n=2-6)$ clusters using density-functional theory (DFT) methods. Song and co-workers[24,25] computed geometries and energetics of all the nonstochiometeric clusters containing three to eight atoms with the full-potential linear-muffin-tin-orbital molecular-dynamics (FP-LMTO MD) method.

There have been four theoretical studies dealing directly with Ga_2N and its anion. In a series of papers by Kandalam *et al.*[21] and Costales *et al.*,[22] the structures, vibrational frequencies, energetics, and electron densities of Ga_2N and Ga_2N^+ were calculated using the nonlocal-density approximation to the density-functional theory. A linear $D_{\infty h}$ structure for Ga_2N was found to have the lowest energy, although this structure had an imaginary frequency. Based on comparison with Al_2N, a nearly isoenergetic quasilinear C_{2v} structure with a Ga–N–Ga angle of 172° and Ga–N bond length of 1.79 Å was predicted to be ground state. Song and Cao[25] also predicted the lowest-energy structure to have C_{2v} symmetry with a Ga–N–Ga angle of 157.87° and Ga–N bond length of 1.80 Å. Most recently, Wang and Balasubramanian[26] reported a study on the ground state of the anion and neutral as well as several excited states of the neutral. They investigated geometries, frequencies, and energetics using DFT, Moller-Plesset perturbation theory with second-order electron correlation (MP2), coupled cluster double excitation (CCD), complete active space multicon-

[a]Present address: Sandia National Laboratories, Mail Stop 9055, Livermore, CA 94550.
[b]Author to whom correspondence should be addressed. Electronic mail: dneumark@berkeley.edu

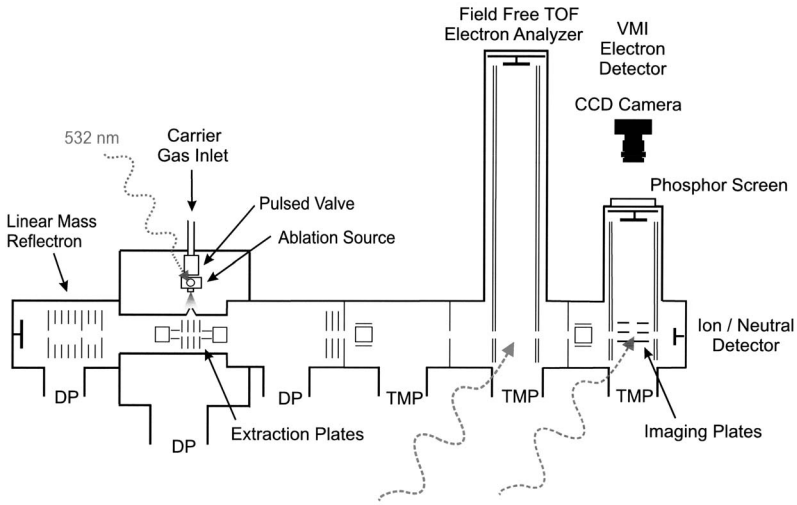

FIG. 1. Schematic drawing of the photoelectron spectrometer incorporating the new velocity-map imaging (VMI) setup.

figuration self-consistent field (CASSCF), and multireference singles plus doubles configuration interaction (MRSDCI) calculations. In each case, the ground state of the neutral was calculated to be a linear $D_{\infty h}(^2\Sigma_u^+)$ structure with Ga–N bond lengths ranging from 1.725 to 1.778 Å. The anion ground state was predicted to have a linear $D_{\infty h}(^1\Sigma_g^+)$ structure. Two doublet neutral excited states were also calculated to be linear $D_{\infty h}$ structures.

The only previous experimental work pertaining to the spectroscopic characterization of small gallium nitride clusters was performed by Zhou and Andrews,[27] who carried out a combined theoretical/experimental study using DFT methods and matrix isolation infrared spectroscopy. GaN, Ga_2N, Ga_3N, GaN_2, and GaN_3 clusters were produced by reaction of laser-ablated gallium atoms with isotopic mixtures of N_2 gas. Their DFT calculations of the ground state of Ga_2N gave a $^2\Sigma_u^+$ linear $D_{\infty h}$ structure with Ga–N bond lengths of approximately 1.79 Å in agreement with those of Wang and Balasubramanian. A weak band at 757.4 cm^{-1} was tentatively assigned as the antisymmetric stretching frequency based on comparison of isotopic ratios and a calculated frequency of approximately 867 cm^{-1}.

In this paper, we present the PE spectra of Ga_2N^- at photodetachment laser wavelengths of 416, 355, and 266 nm and report on the spectroscopic properties of the neutral ground state and the first excited state. In the next section we give a brief explanation of the experimental setup used in this study. Section III discusses the main features of the spectra, and Sec. IV provides a detailed discussion of the results.

II. EXPERIMENT

The anion photoelectron spectrometer used in this experiment, which has been described in detail previously,[28,29] has recently been upgraded by the incorporation of a PE imaging system, in addition to the field-free time-of-flight (TOF) electron detection scheme already present. The current version of the spectrometer is shown in Fig. 1.

Ga_2N^- anions were generated by pulsed laser ablation of a rotating solid gallium nitride target with the second harmonic (532 nm, 30–40 mJ/pulse) of a neodymium-doped yttrium aluminum garnet (Nd:YAG) laser. The gallium nitride disks were prepared from 99.99% pure powder (Aldrich) in a 200 000 psi isostatic press. The resulting plasma was entrained in a pulsed jet of carrier gas. The expansion passed through a skimmer into a differentially pumped region where the negative ions were perpendicularly extracted by pulsed electric fields and accelerated to a final energy of 2.5 keV. The anions were focused and separated by mass-to-charge ratio in a linear reflectron time-of-flight mass spectrometer. The mass resolution is estimated to be $m/\Delta m=2000$.

Both N_2 and Ar were used as expansion gases in this experiment with typical backing pressures from 15–20 psi(gauge). Using neat N_2 or Ar, the dominant species in the mass spectra were gallium metal clusters and their oxides. The presence of oxides is a result of oxidation of the GaN powder before being pressed into a disk. In order to reduce the amount of oxides, the backing gas was bubbled through aqueous NH_4OH to seed NH_3 in the molecular beam. The addition of NH_3 effectively reduced $Ga_xO_y^-$ clusters with the exception of GaO^-. It also enhanced the formation of Ga_xN^- clusters. Gallium-rich clusters are expected to be the most abundant species in the ablation plume due to the high surface temperatures of the disk during ablation and the ease of boiling off stable N_2 molecules. Ga_2N^- was the most intense $Ga_xN_y^-$ cluster in the mass spectra. No stoichiometric clusters were observed, although Ga_xN_x ($x=1-6$) are expected to have positive electron affinities ranging from 1.2–2.5 eV.[16,18] The Ga_2N^- peaks comprise a triplet in the mass spectrum owing to the isotopic abundances of Ga (60% ^{69}Ga and 40% ^{71}Ga). The absence of Ga_2O^- was confirmed by a lack of signal for the 158 amu ($^{71}Ga_2O$) peak. All spectra were taken from photodetachment of the most intense peak of the Ga_2N^- triplet at 154 amu ($^{69}Ga^{71}GaN^-$).

Mass-selected anions were photodetached at the spatial focus of either the field-free TOF photoelectron detector or the PE imaging detector with various wavelengths obtained from an Nd:YAG laser. We used the third (355 nm, 3.493 eV) and fourth (266 nm, 4.661 eV) harmonics of the Nd:YAG laser. Additionally, we generated 416 nm (2.978 eV) photons by Raman shifting the third harmonic of the Nd:YAG in a 325 psi(gauge) H_2 cell.

In the field-free TOF electron detection scheme, photo-

electrons are detected using a microchannel plate (MCP) detector in a chevron configuration at the end of a 1 m field-free flight tube oriented perpendicular to the laser-beam and molecular-beam axes. The electrons are energy analyzed by TOF with an energy resolution of 8–10 meV at 0.65 eV of electron kinetic energy (eKE), which degrades as $e\mathrm{KE}^{3/2}$ for higher eKE.

The imaging technique we use is based on that of Chandler and Houston[30] with the velocity-map imaging (VMI) modification of Eppink and Parker.[31] The imaging setup is very similar to that of Sanov[32] and Lineberger[33] in that the electrons are extracted by the imaging fields perpendicularly to both the laser and ion beams. The imaging stack is oriented vertically and consists of three 4.5 in. diameter stainless steel plates evenly spaced by 2 cm. The ion beam passes between the center of the bottom (repeller) and middle (extractor) plates. Voltages are applied to the repeller and extractor, while the upper plate is held at ground. The aperture of the middle and upper plates is 2.0 cm in diameter. The electrons are detected at the end of a 30 cm double μ-metal-shielded flight tube by a 75 mm chevron MCP stack coupled to a phosphor screen (Burle Electro-Optics, Inc.). An externally triggered CCD camera (Dalsa) records one image per laser shot at 20 Hz. Typically images were summed for 10–50 000 laser shots compared to 150–300 000 for field-free TOF spectra.

Focusing, calibration, and energy resolution of the VMI assembly were determined using O_2^- or I^-, for which the electron binding energies are well known.[34,35] The voltage ratio between the extractor and repeller giving optimal focusing conditions was found to be around 0.7. After focusing and acquisition, the three-dimensional image was reconstructed from the raw two-dimensional image by the basis-set expansion (BASEX) Abel transform method developed by Dribinski *et al.*[36] The central two-dimensional slice of the reconstructed three-dimensional image was angularly integrated to obtain a velocity space spectrum which is then converted to eKE. The conversion factor was obtained by calibrating the instrument at the given wavelength and voltage set. The best energy resolution obtained so far corresponds to a $\Delta E/E$ of approximately 0.02.

The angular distribution of photoelectrons is given by

$$\frac{d\sigma}{d\Omega} = \frac{\sigma_{\mathrm{total}}}{4\pi}\left[1 + \frac{\beta}{2}(3\cos^2\theta - 1)\right], \tag{1}$$

where θ is the angle between the laser electric field and the electron TOF axis, σ_{total} is the total photodetachment cross section, and β is the anisotropy parameter which varies from -1 to 2.[37] Each neutral $\leftarrow$ anion electronic transition has a characteristic β that can be used to distinguish peaks of overlapping electronic transitions. Although the field-free technique offers somewhat better resolution, the VMI data provides more accurate anisotropy parameters with significantly fewer laser shots. Anisotropy parameters for given peaks were determined from the image by fitting electron intensity as function of θ to Eq. (1).

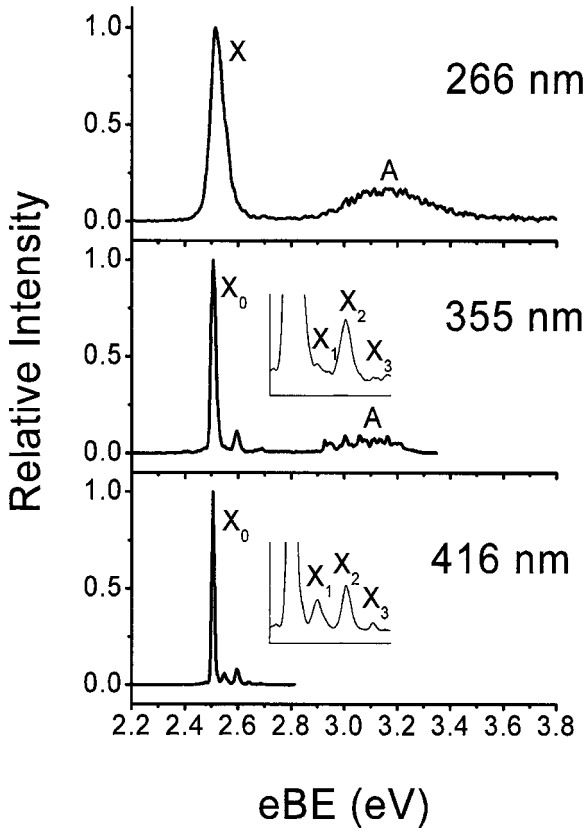

FIG. 2. Field-free TOF photoelectron spectra of Ga_2N^- using 416, 355, and 266 nm at $\theta=0°$ plotted as eBE (eV) vs relative intensity.

III. RESULTS

A. Photoelectron spectra

The 416, 355, and 266 nm PE spectra of Ga_2N^- obtained from field-free TOF with $\theta=0°$ (in order to maximize signal) are displayed in Fig. 2. All PE spectra in this work are shown with the most intense feature scaled to unity and are plotted as relative intensity versus electron binding energy (eBE) in units of eV, where

$$e\mathrm{BE} = h\nu - e\mathrm{KE} = \mathrm{EA} + E^0 - E^{(-)}. \tag{2}$$

Here $h\nu$ is the photon energy, eKE is the electron kinetic energy, EA is the adiabatic electron affinity, E^0 is the internal energy of the neutral, and $E^{(-)}$ is the internal energy of the anion. The spectra in Fig. 2 are plotted from 2.2 to 3.8 eV and no other features were observed at lower eBE. A spectrum at 213 nm (5.821 eV, not shown) revealed no additional peaks. A VMI image showing raw (left half) and transformed (right half) data is shown in Fig. 3. The image was taken at 355 nm and the electric-field vector is vertical with respect to the image. Figure 4 is a comparison plot of the 355 nm PE spectra obtained from the field-free TOF detector at $\theta=0°$ and from the VMI image.

The 266 nm spectrum in Fig. 2 (top) consists of two well-separated features, band X and band A, with maximum intensities at approximately 2.5 and 3.2 eV, respectively. Both the X and A bands are also present in the 355 nm spectrum [Figs. 2 (middle) and 3], while only the X band is present in the 416 nm spectrum [Fig. 2 (bottom)]. In both 416 and 355 nm spectra, band X is resolved into four peaks,

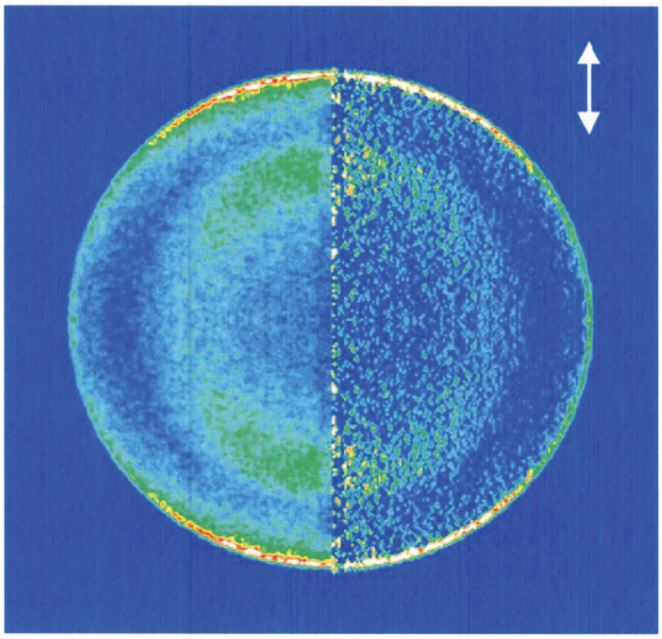

FIG. 3. (Color) Raw (left half) and BASEX-transformed (right half) VMI image of Ga_2N^- summed over 40 000 laser shots at 355 nm. The laser polarization is vertical in the image.

X_0 through X_3. Band A in the 355 nm field-free TOF spectrum has more resolved features than the 266 nm spectrum, reflecting the degradation in resolution with increasing eKE as discussed previously.

Band X, assumed to be the transition between anion and neutral ground states, is dominated by a single intense peak X_0 with several smaller peaks at higher binding energy. We assign X_0 to the vibrational band origin and the smaller peaks to transitions to vibrationally excited levels of Ga_2N. The absence of an extended vibrational progression indicates a small change in geometry between the anion and neutral states. Table I lists peak positions within band X for both the 416 and 355 nm spectra in eBE. ΔE represents the approximate separation between each peak and X_0 in cm^{-1}. Anisotropy parameters for selected peaks derived from the VMI

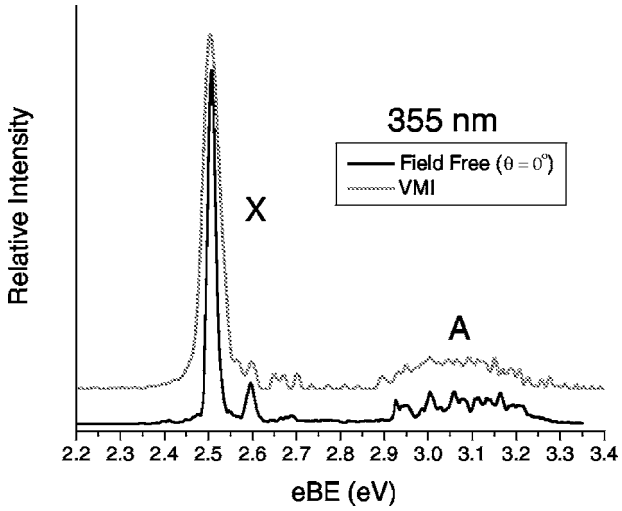

FIG. 4. Comparison of the $\theta=0°$ field-free TOF and the VMI photoelectron spectra at 355 nm.

TABLE I. Peak positions within band X in eBE (eV) for both the 416 and 355 nm field-free TOF spectra. ΔE is the energy difference between the peak and the origin peak in cm^{-1}. Also shown are the anisotropy parameters obtained from the VMI image at 355 nm.

	eBE (eV)			
Peak	416 nm	355 nm	ΔE (cm^{-1})	β_{VMI} 355 nm
X_0	2.506	2.507	0	1.0
X_1	2.549	2.550	345	1.0
X_2	2.598	2.599	740	0.3
X_3	2.641	2.642	1085	

data are also given. X_0 has an eBE of approximately 2.5 eV in both the 416 and 355 nm spectra. The X_0-X_1 spacing is approximately 345 cm^{-1} in both the 416 and 355 nm spectra. The X_0-X_2 spacing is approximately 740 cm^{-1}. The X_0-X_3 spacing is approximately 1085 cm^{-1} in both the 416 and 355 nm spectra. The anisotropy parameter β is 1.0 for peaks X_0 and X_1, but is considerably lower (0.3) for peak X_2. The anisotropy parameter for peak X_3 could not be obtained due to its low intensity.

Band A is less intense and more extended than band X, indicating a relatively large change in geometry between the anion and neutral states. It is assigned as the transition between the anion ground state and the first excited electronic state of the neutral. The best resolution of band A occurs in the 355 nm spectrum. The number and unequal spacing of the peaks indicate that this band is composed of vibrational progressions in at least two modes. A series of some of the most intense peaks is spaced by approximately 447 cm^{-1}. Identification of the origin peak is not as straightforward as in band X, and Franck-Condon (FC) simulations are needed as will be discussed in Sec. IV. We note that the Ga_2N^- PE spectra are similar in appearance to those recently measured for Al_2N^-, with a well-resolved ground-state band and poorly resolved excited-state bands.[38]

B. Electronic structure calculations

As stated in the introduction, calculations have been performed previously on the Ga_2N anion[26] and neutral[21,22,25,27] ground states as well as several excited states of the neutral.[26] It is useful to use calculated anion and neutral frequencies and geometries as a starting point in the FC simulations of the PE spectra. However, these simulations require normal coordinate displacements between the anion and neutral electronic states. The force constants used to calculate these displacements are typically not reported, so we carried out our own DFT calculations using the Becke-3-parameter-Lee-Yang-Parr (B3LYP) exchange-correlation functional.[39,40] Our calculations employed the augmented correlation consistent polarized valence double-ζ (aug-cc-pVDZ) basis sets of Dunning[41] and Kendall *et al.*[42] All computations were carried out with the GAUSSIAN 03 program.[43] Based on previous calculations, only $D_{\infty h}$ and C_{2v} starting geometries were optimized.

Results of our calculations are summarized in Table II. Results previously reported by Wang and Balasubramanian[26] at the B3LYP and CCD levels of theory are also shown for

TABLE II. DFT and CCD calculations for the anion and neutral electronic states of Ga_2N. υ_1 corresponds to the symmetric strecth, υ_2 is the bending vibration, and υ_3 is the antisymmetric stretch.

Species	State	Method	Energy (eV)	r_{Ga-N} (Å)	$\upsilon_1(\sigma_g)$ (cm^{-1})	$\upsilon_2(\pi_u)$ (cm^{-1})	$\upsilon_3(\sigma_u)$ (cm^{-1})
Ga_2N^-	$^1\Sigma_g^+$	B3LYP[a]	−2.36	1.797	304	34	987
		B3LYP[b]	−1.99	1.793	305	62	990
		CCD[b]	−1.80	1.749			
Ga_2N	$^2\Sigma_u^+$	B3LYP[a]	0.00	1.784	301	58	878
		B3LYP[b]	0.00	1.778	302	87	889
		CCD[b]	0.00	1.736	331	53	830
	$^2\Pi_u$	B3LYP[a]	0.37	1.923	245	45[c]	749
		B3LYP[b]	0.42	1.913	247	68[c]	750
		CCD[b]	0.30	1.865			
	$^2\Sigma_g^+$	B3LYP[a]	2.06	1.741	355	262	1307
		B3LYP[b]	2.10	1.735	355	273	1293
		CCD[b]	2.07	1.705			

[a]This work.
[b]Wang and Balasubramanian (Ref. 26).
[c]Mean harmonic frequency.

comparison. Table II shows relative energies, geometries, and vibrational frequencies for the ground state of the anion and three states of the neutral. Our calculated frequencies and geometries are in good agreement with the B3LYP and CCD calculations of Wang and Balasubramanian, who used relativistic effective core potentials with valence Gaussian basis sets. Their MP2, CASSCF, and MRSDCI calculations were also in agreement with the B3LYP and CCD results but did not include vibrational frequencies, so they are not shown here. The ground state of the neutral was calculated to be linear ($^2\Sigma_u^+$) in agreement with calculations by Zhou and Andrews.[27] Two doublet excited states of the neutral were also linear ($^2\Pi_u$ and $^2\Sigma_g^+$) as well as the anion ground state ($^1\Sigma_g^+$). Note the extremely low bending frequencies for the anion and lowest two neutral states. The triplet states of the anion and quartet states of the neutral lie several eV higher in energy than the corresponding singlet and doublet states and are not listed in Table II.

IV. DISCUSSION

It can be reasonably assumed that all of the anions generated in the supersonic expansion will reside in the ground electronic state $X\ ^1\Sigma_g^+$, since we calculated the nearest triplet excited state to be nearly 2.5 eV higher in energy. Accordingly, band X is the transition between the ground state of the anion and the ground state of the neutral ($X\ ^2\Sigma_u^+ \leftarrow X\ ^1\Sigma_g^+$). The position of peak X_0 gives the electron affinity for Ga_2N, 2.506±0.008 eV. Peak X_1 is assigned to the $\upsilon=1$ level of the symmetric stretch υ_1 (σ_g) mode of the neutral with a frequency of 345±40 cm^{-1}. This value is in good agreement with the CCD calculation of Wang and Balasubramanian of 331 cm^{-1} but is slightly higher than our B3LYP value of 301 cm^{-1} and that of Wang and Balasubramanian of 302 cm^{-1}. The X_2-X_0 spacing, 740±40 cm^{-1}, agrees with the matrix IR frequency of 757.4 cm^{-1} assigned to the antisymmetric stretch by Zhou and Andrews.[27] We assign peak X_2 to the $\upsilon=1$ level of the antisymmetric stretch υ_3 (σ_u) mode. This value is, however, at least 100 cm^{-1} lower than the calculated frequencies in Table II, a point discussed in more detail below. Peak X_3 is assigned to the $\upsilon_1+\upsilon_3$ combination band with a frequency of 1085 cm^{-1}. No anion frequencies were obtained from the spectra owing to the low intensity of the hot bands.

Nontotally symmetric modes such as the υ_3 mode generally show little FC activity in a PE spectrum, but when they do, only even $\Delta\upsilon$ transitions are allowed. Hence, the appearance of peak X_2 cannot be explained by simple Franck-Condon arguments. Its much lower anisotropy parameter (0.3) compared to X_0 and X_1 (1.0) suggests it arises from vibronic coupling to an excited neutral electronic state, as was seen in the PE spectra of B_2N^- (Ref. 44) and Al_2N^-.[38] Peak X_2 can borrow intensity from an excited-state vibrational level with the same overall vibronic symmetry ($\Sigma_u^+ \otimes \sigma_u = \Sigma_g^+$) such as σ_g vibrational levels of a $^2\Sigma_g^+$ state, and this coupling should produce anisotropy parameters similar to those of the excited state.[44,45] We calculate a $^2\Sigma_g^+$ excited state to lie 2.1 eV above the ground state. However, we do not observe this state, even in a PE spectrum taken at 213 nm (5.821 eV). In contrast, the $^2\Sigma_g^+$ first excited state of B_2N was observed to be only 0.785 eV above the ground state and the anisotropy parameters of the odd levels of the υ_3 mode ($\upsilon=1$ and 3) clearly tracked with this upper state.

The calculated frequencies for the υ_3 mode of the neutral ground state are 138 and 149 cm^{-1} higher than our experiment in B3LYP and the B3LYP calculation of Wang and Balasubramanian, respectively, and 90 cm^{-1} higher in the CCD calculations of Wang and Balasubramanian. A similar effect was observed in the case of B_2N^-, where the observed fundamental for the antisymmetric stretch was 36% lower than the calculated B3LYP value. Additionally, the progression in B_2N showed a large negative anharmonicity. Both effects could be reproduced assuming a linear vibronic coupling model between the ground and excited states of B_2N.[46] In our case, the υ_3 progression is not extended enough to warrant such a treatment.

In order to interpret the PE spectra and yield more accurate values for electron affinities, term energies, and vibra-

TABLE III. Best-fit parameters for the simulations of band *X* at 416 nm and band *A* at 355 nm. Frequencies and normal coordinate displacements are given for each band.

Band	Wavelength	*e*BE (eV)	υ (cm^{-1})	ΔQ (Å $amu^{1/2}$)	Δr (Å)	Assignment
X	416 nm	2.506	345	0.120	−0.014	$\upsilon_1(\sigma_g)$
			740			$\upsilon_3(\sigma_u)$
A	355 nm	2.950	447	0.600	0.072[a]	
			622	0.250		

[a]Assumes that this vibration is assigned to the symmetric stretch of the $^2\Pi_u$ state.

tion frequencies, FC simulations of the spectra were carried out for each electronic transition. Calculated geometries and frequencies were used as a starting point for each of the simulations. Vibrational frequencies, normal coordinate displacements, and detachment energies were adjusted iteratively to obtain fits to the spectra. Only the higher-resolution, field-free TOF spectra were used in the fitting. Table III summarizes the results of the simulations for band *X* at 416 nm and band *A* at 355 nm. The FC simulation of band *X* at 416 nm appears in Fig. 5, and simulations of band *A* at 355 nm appear in Fig. 6. The temperature used for the simulations was 300 K.

In the FC simulation, normal coordinate displacements between the anion and neutral vibrational modes are used as input parameters. These parameters are used to vary the length and intensity pattern of vibrational progressions in the simulated spectra. Once a spectrum is fit, these values can be used to calculate the relative changes in geometry between the anion and neutral. Under the FC approximation, normal coordinate displacements for the antisymmetric stretch ΔQ_3 are zero for transitions between linear centrosymmetric structures, and the normal coordinate displacement for the symmetric stretch (ΔQ_1) is used exclusively to determine the bond distance change.

According to the FC simulation of band *X*, the Ga–N bond distance changes by 0.014±0.005 Å between the anion and neutral ground states. Based on calculations, the sign of this change is expected to be negative upon photodetachment. The highest occupied molecular orbital (HOMO) of the anion $^1\Sigma_g^+$ state is doubly occupied with σ_u symmetry and appears to be slightly antibonding. It is composed of mainly *s* and p_z atomic orbitals on the Ga atoms and almost exclusively p_z orbitals on the central nitrogen. Our B3LYP result and the CCD result of Wang and Balasubramanian both predict a shortening of the Ga–N bond by 0.013 Å. The B3LYP calculation by Wang and Balasubramanian gives a 0.015 Å decrease. The CASSCF method used by Wang and Balasubramanian predicts a much larger change in r_{Ga-N} of −0.110 Å between anion and neutral.

Based on the calculated energetics, band *A* appears to be a transition between the anion ground state and the first excited state of the neutral ($A\ ^2\Pi_u \leftarrow X\ ^1\Sigma_g^+$). A simulated spectrum based on our B3LYP frequencies and normal coordinate displacements for the $A\ ^2\Pi_u \leftarrow X\ ^1\Sigma_g^+$ transition, which yields only a single progression in the υ_1 symmetric stretch, is shown in Fig. 6 (light gray fill). The fit gave poor agreement with the 355 nm spectrum (dark gray fill), although the envelope of the band at 355 nm is fairly well reproduced. A better fit to the data was achieved assuming two active modes with frequencies of 447±40 and 622±40 cm^{-1} originating at an *e*BE of 2.950±0.055 eV (Fig. 6, black line). The uncertainty of this origin remains large, and the error bar corresponds to one quantum of the lower vibrational frequency. Shifting the simulated spectrum by ±447 cm^{-1} gave reasonable fits, although not as good as the unshifted spectrum. The poor fit of the simulation toward high *e*BE is presumably a result of a diminishing cross section near thresh-

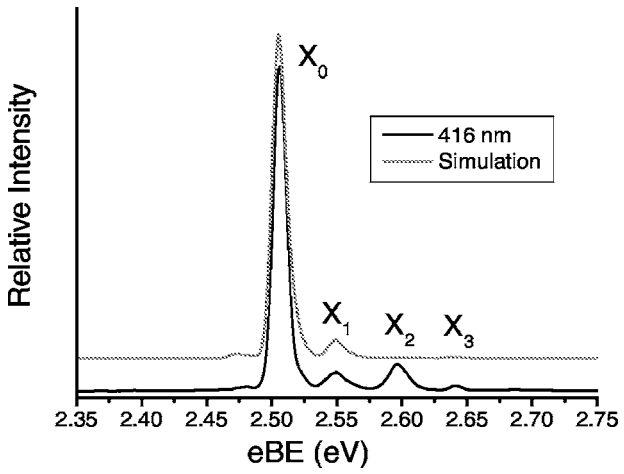

FIG. 5. FC simulation of band *X* at 416 nm.

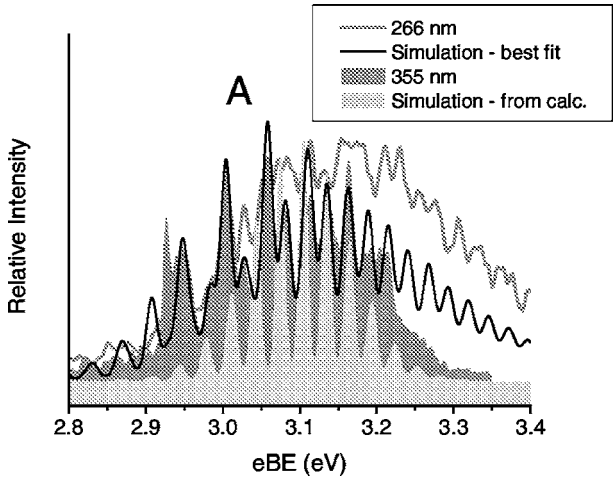

FIG. 6. FC simulations of band *A* at 355 nm (dark gray fill) using the values obtained from our B3LYP calculations (light gray fill) and the best-fit values (black line). Also shown for comparison is the 266 nm spectrum (dark gray line).

old, as can be seen by comparison with the 266 nm spectrum (Fig. 6, dark gray line). However, our calculated B3LYP frequency for the symmetric stretch of the $^2\Pi_u$ state (245 cm^{-1}) is 202 cm^{-1} below the lower simulated frequency, while our B3LYP value for the antisymmetric stretch of the $^2\Pi_u$ state (749 cm^{-1}) is 127 cm^{-1} above the higher simulated frequency. Assuming 447 cm^{-1} is the symmetric stretch frequency of the $^2\Pi_u$, the normal coordinate displacement obtained from the best-fit simulation is also not consistent with the calculations. The simulated ΔQ_1 from the 355 nm spectrum gives a change in bond length of 0.072 Å between the anion $^1\Sigma_g^+$ state and the neutral $^2\Pi_u$ state. Our B3LYP calculation gives almost double this value at 0.126 Å.

The discrepancies between the best-fit simulation and calculations suggest that there are some effects not accounted for in the calculations. Presuming the upper state of band *A* is linear and centrosymmetric, only the symmetric stretch should be active and a vibronic coupling argument would have to be invoked to account for the appearance of an antisymmetric stretching mode. If the upper state was actually bent with C_{2v} symmetry instead of linear, both a bending and symmetric stretches would be expected to be active. The bending and symmetric stretch frequencies would then be 447 and 622 cm^{-1}, respectively. Overall, the assignment of band *A* to the linear $^2\Pi_u$ state is supported by the energetics but not by simulations of its vibrational structure.

V. CONCLUSIONS

Anion PE spectra of Ga_2N^- at 416, 355, and 266 nm using both field-free TOF and VMI techniques are presented. The spectra show transitions to two electronic states of the neutral. The spectra are discussed in detail and analyzed with the aid of electronic structure calculations and FC simulations. Band *X* is assigned to the transition from the anion ground state to neutral ground state $X\,^2\Sigma_u^+ \leftarrow X\,^1\Sigma_g^+$, yielding the first experimental determination of the EA for Ga_2N. The vibrational frequencies for the symmetric and antisymmetric stretching modes of the neutral ground state were also obtained as well as the relative geometry change for the transition. A breakdown of the FC principle due to vibronic coupling was observed in the antisymmetric stretch.

A second partially vibrationally resolved band was also observed in the 355 and 266 nm spectra. Vibrational frequencies were obtained from a best-fit FC simulation but were not matched with calculated frequencies. The energy of this band is consistent with the $A\,^2\Pi_u^+ \leftarrow X\,^1\Sigma_g^+$ transition, but its congested appearance is more consistent with a transition to a bent neutral state.

ACKNOWLEDGMENT

The authors acknowledge the financial support of the National Science Foundation under Grant No. DMR-0505311.

[1] S. Nakamura, T. Mukai, and M. Senoh, Jpn. J. Appl. Phys., Part 2 **30**, L1998 (1991).
[2] S. Nakamura, N. Senoh, N. Iwasa, and S. I. Nagahama, Jpn. J. Appl. Phys., Part 2 **34**, L797 (1995).
[3] S. Nakamura, M. Senoh, S. Nagahama, N. Iwasa, T. Yamada, T. Matsushita, H. Kiyoku, and Y. Sugimoto, Jpn. J. Appl. Phys., Part 2 **35**, L74 (1996).
[4] S. Nakamura, M. Senoh, S. Nagahama, N. Iwasa, T. Yamada, T. Matsushita, H. Kiyoku, and Y. Sugimoto, Jpn. J. Appl. Phys., Part 2 **35**, L217 (1996).
[5] Y. Huang, X. F. Duan, Y. Cui, and C. M. Lieber, Nano Lett. **2**, 101 (2002).
[6] J. C. Johnson, H. J. Choi, K. P. Knutsen, R. D. Schaller, P. D. Yang, and R. J. Saykally, Nat. Mater. **1**, 106 (2002).
[7] K. M. Ervin and W. C. Lineberger, in *Advances in Gas Phase Ion Chemistry*, edited by N. G. Adams and L. M. Babcock (JAI, Greenwich, CT, 1992), Vol. 1, pp. 121–166.
[8] K. R. Asmis, T. R. Taylor, and D. M. Neumark, Chem. Phys. Lett. **308**, 347 (1999).
[9] T. R. Taylor, H. Gomez, K. R. Asmis, and D. M. Neumark, J. Chem. Phys. **115**, 4620 (2001).
[10] H. Gomez, T. R. Taylor, and D. M. Neumark, J. Phys. Chem. A **105**, 6886 (2001).
[11] G. Meloni, M. J. Ferguson, S. M. Sheehan, H. Gomez, Z. Liu, and D. M. Neumark, Chem. Phys. Lett. **392**, 90 (2004).
[12] J. J. BelBruno, Heteroat. Chem. **11**, 281 (2000).
[13] A. K. Kandalam, M. A. Blanco, and R. Pandey, J. Phys. Chem. B **105**, 6080 (2001).
[14] B. Song and P. L. Cao, Phys. Lett. A **300**, 485 (2002).
[15] B. Song and P. L. Cao, Phys. Lett. A **306**, 57 (2002).
[16] A. Costales and R. Pandey, J. Phys. Chem. A **107**, 191 (2003).
[17] A. K. Kandalam, M. A. Blanco, and R. Pandey, J. Phys. Chem. B **106**, 1945 (2002).
[18] A. Costales, A. K. Kandalam, and R. Pandey, J. Phys. Chem. B **107**, 4508 (2003).
[19] B. Song and P. L. Cao, Chin. Phys. Lett. **20**, 1488 (2003).
[20] L. T. Ueno, O. Roberto-Neto, S. Canuto, and F. B. C. Machado, Chem. Phys. Lett. **413**, 65 (2005).
[21] A. K. Kandalam, R. Pandey, M. A. Blanco, A. Costales, and J. M. Recio, J. Phys. Chem. B **104**, 4361 (2000).
[22] A. Costales, A. K. Kandalam, A. M. Pendas, M. A. Blanco, J. M. Recio, and R. Pandey, J. Phys. Chem. B **104**, 4368 (2000).
[23] A. Costales, M. A. Blanco, A. M. Pendas, A. K. Kandalam, and R. Pandey, J. Am. Chem. Soc. **124**, 4116 (2002).
[24] B. Song, L. Ling, and P. L. Cao, Chin. Phys. **13**, 489 (2004).
[25] B. Song and P. L. Cao, Phys. Lett. A **328**, 364 (2004).
[26] C. S. Wang and K. Balasubramanian, Chem. Phys. Lett. **402**, 294 (2005).
[27] M. F. Zhou and L. Andrews, J. Phys. Chem. A **104**, 1648 (2000).
[28] R. B. Metz, A. Weaver, S. E. Bradforth, T. N. Kitsopoulos, and D. M. Neumark, J. Phys. Chem. **94**, 1377 (1990).
[29] C. S. Xu, G. R. Burton, T. R. Taylor, and D. M. Neumark, J. Chem. Phys. **107**, 3428 (1997).
[30] D. W. Chandler and P. L. Houston, J. Chem. Phys. **87**, 1445 (1987).
[31] A. T. J. B. Eppink and D. H. Parker, Rev. Sci. Instrum. **68**, 3477 (1997).
[32] E. Surber, R. Mabbs, and A. Sanov, J. Phys. Chem. A **107**, 8215 (2003).
[33] G. J. Rathbone, T. Sanford, D. Andrews, and W. C. Lineberger, Chem. Phys. Lett. **401**, 570 (2005).
[34] K. M. Ervin, W. Anusiewicz, P. Skurski, J. Simons, and W. C. Lineberger, J. Phys. Chem. A **107**, 8521 (2003).
[35] D. Hanstorp and M. Gustafsson, J. Phys. B **25**, 1773 (1992).
[36] V. Dribinski, A. Ossadtchi, V. A. Mandelshtam, and H. Reisler, Rev. Sci. Instrum. **73**, 2634 (2002).
[37] J. Cooper and R. N. Zare, J. Chem. Phys. **48**, 942 (1968).
[38] G. Meloni, S. M. Sheehan, B. F. Parsons, and D. M. Neumark, J. Phys. Chem. A (in press).
[39] C. T. Lee, W. T. Yang, and R. G. Parr, Phys. Rev. B **37**, 785 (1988).
[40] A. D. Becke, J. Chem. Phys. **98**, 1372 (1993).
[41] T. H. Dunning, J. Chem. Phys. **90**, 1007 (1989).
[42] R. A. Kendall, T. H. Dunning, and R. J. Harrison, J. Chem. Phys. **96**, 6796 (1992).
[43] M. J. Frisch, G. W. Trucks, H. B. Schlegel *et al.*, GAUSSIAN 03, Revision C.02, Gaussian Inc., Wallingford, CT, 2004.
[44] K. R. Asmis, T. R. Taylor, and D. M. Neumark, J. Chem. Phys. **111**, 8838 (1999).
[45] K. M. Ervin and W. C. Lineberger, J. Phys. Chem. **95**, 1167 (1991).
[46] F. Tarantelli, L. S. Cederbaum, and P. Campos, J. Chem. Phys. **91**, 7039 (1989).